Published in final edited form as:
Anat Rec A Discov Mol Cell Evol Biol. 2006 April ; 288(4): 397–408. doi:10.1002/ar.a.20300.

Projections from Auditory Cortex to Cochlear Nucleus: A Comparative Analysis of Rat and Mouse

Noah E. Meltzer[1] and **David K. Ryugo**[1,2]

[1]Center for Hearing and Balance, Department of Otolaryngology-HNS, Johns Hopkins University School of Medicine, Baltimore, MD 21205

[2]Center for Hearing and Balance, Department of Neuroscience, Johns Hopkins University School of Medicine, Baltimore, MD 21205

Abstract

Mammalian hearing is a complex special sense that involves detection, localization, and identification of the auditory stimulus. The cerebral cortex may subserve higher auditory processes by providing direct modulatory cortical projections to the auditory brainstem. To support the hypothesis that corticofugal projections are a conserved feature in the mammalian brain this manuscript reviews features of the rat corticofugal pathway and presents new data supporting the presence of similar projections in the mouse. The mouse auditory cortex was localized with electrophysiological recording and neuronal tracers were injected into A1. The cochlear nucleus was dissected and examined for terminal fibers by light and electron microscopy. Bouton endings were found bilaterally forming synapses with dendrites of granule cells of the cochlear nucleus. This report provides evidence for direct auditory cortex projections to the cochlear nucleus in the mouse. The distribution of projections to the granule cell domain and the synapses onto granule cell dendrites are consistent with what has been reported for rats and guinea pigs. These findings suggest a general plan for corticofugal modulation of ascending auditory information in mammals. Corticobulbar inputs to the auditory brainstem likely provided a survival advantage by improving sound detection and identification, thus allowing the development of complex social behaviors and the navigation of varied environments.

Keywords

corticobulbar; auditory; mouse; cochlear nucleus; granule cell

The growth of the cerebral cortex is one key to evolutionary success. The cerebral cortex and its interconnected structures grow substantially as one ascends the phylogenetic tree (Fig. 1). The corticofugal system—descending inputs from cerebral cortex to lower brain centers—may grow in parallel and its presence in the neural network presumably contributes to the refinement and enhancement of behavior. The selective listening feature of hearing must have structural components, one of which may be the direct influence of auditory cortex on the first central auditory station, the cochlear nucleus. It is our working hypothesis that further description and functional characterization of these circuits will eventually form the foundation for our understanding of hearing. This manuscript presents experimental data demonstrating cortico-cochlear nucleus projections in the mouse. In order to place these findings in the context of a general plan for cortical modulation of mammalian auditory function we review our prior studies on cortical projections to the cochlear nucleus in rats.

Corresponding author: David K. Ryugo, Center for Hearing and Balance, Johns Hopkins University School of Medicine, 720 Rutland Ave., Baltimore, MD 21205, Telephone 410-955-4543, Facsimile 410-614-4748, e-mail dryugo@bme.jhu.edu.

These findings demonstrate a conserved template for cortical modulation of auditory information at the level of the cochlear nucleus in rodents.

Cortical Projections to the Cochlear Nucleus

Although it had long been known that somatosensory cortex projected to sensory relay nuclei of the medulla (Weisberg and Rustioni, 1976, 1977, 1979), more recent studies showed a parallel projection from auditory cortex to the cochlear nucleus (Feliciano et al., 1995; Weedman and Ryugo, 1996). These anterograde tracer experiments revealed a strong bilateral projection from auditory cortex to the granule cell domain (GCD). The GCD is a region of the cochlear nucleus characterized by neurons with small cell bodies, strong histochemical presence of acetylcholinesterase, and no staining of myelinated fibers. These small cells, however, are not homogeneous (Mugnaini et al., 1980a,b; Floris et al., 1994; Weedman et al., 1996). Most of the cells are granule cells, characterized by small cell bodies and 1–4 primary dendrites with a distinct terminal claw. Hair-like appendages grow out of the tips of these claws. Also present are unipolar brush cells, with their single, stout primary dendrite with a dense snarl of branches, and chestnut cells that lack dendrites altogether. At first glance, these cells represent the main source of potential targets of the corticobulbar projections.

Identification of Corticobulbar Projections in Rat

A first step in the process of defining the cellular components of the corticobulbar circuit was to identify the projecting cells. Injections of a retrograde tracer, Fast Blue, were made into the cochlear nucleus (Fig. 2). Retrogradely labeled pyramidal cells were found bilaterally in the deep part of layer V across the caudo-lateral aspect of temporal cortex (Fig. 3). A cyto- and fibroarchtectonic analysis of this cortical region revealed that the labeled cells were restricted to an area of cortex that could be distinguished by a high density of small cells in layer IV and a high density of myelinated fibers (Fig. 4). The surface location of this region coincided with a region characterized electrophysiologically as containing cells with short first spike latencies, sharp tuning, and a tonotopic organization (Sally and Kelly, 1988). These collective features represent criteria for defining the region as primary auditory cortex (Weedman and Ryugo, 1996a;Doucet et al., 2003). These basic results were confirmed recently for the guinea pig (Schofield and Coomes, 2005).

The next step in establishing the corticobulbar circuit was to identify the cellular targets of the pyramidal cells projecting to the cochlear nucleus. Anterograde tracer injections of biotinylated dextran amine into auditory cortex (Te1) demonstrated fine fibers and swellings throughout the granule cell domain of the cochlear nuclei (Fig. 5). Because the data suggested that primary auditory cortex was the sole supplier of these projections (Weedman and Ryugo, 1996a), it was not necessary to worry about spread of the tracer into auditory belt cortex (Weedman and Ryugo, 1996b). Using electron microscopy to elucidate the ultrastructure of the labeled endings, it was shown that the boutons make asymmetrical synapses with thin, irregularly-shaped dendrites (Fig. 6A, B). The thin dendrites are filled with microtubules and the hair-like appendages that penetrate the afferent endings are the defining features of the terminal claw of granule cell dendrites. Labeled boutons filled with round synaptic vesicles terminate on the tip of dendritic claws (Fig. 6C). Corticofugal boutons and terminals filled with pleiomorphic synaptic vesicles converge upon the mossy fiber-dendritic complex and emphasize the complexity of the synaptic neuropil. These data established that the main target of the auditory cortical projection to the cochlear nucleus is a granule cell. The objective of this current set of experiments was to test whether the organization of cortico-cochlear nucleus projections in rats was conserved in another species, namely mice.

Methods

Seven normal hearing adult male CBA/J mice (Jackson Laboratories) were used in this study. All methods used in this report were in accordance with NIH guidelines and approved the Animal Care and Use Committee of the Johns Hopkins University School of Medicine. Each subject in this report had electrophysiologically and histologically confirmed injection sites restricted to AI.

Electrophysiology

General anesthesia was induced and maintained with ketamine and xylazine (IP). Atropine was used to reduce airway secretions, and dexamethasone was used to minimize cerebral edema. The left temporal cortex was exposed using a drill, leaving the dura mater intact. Because the murine cerebral cortex has no landmarks on its surface, we used electrophysiological methods to identify auditory responsive cortex (Fig. 7). Free field auditory stimuli were generated with a software-controlled (MatLab) signal processor (Tucker Davis, Alachua, FL). Recordings were performed using tungsten electrodes (2–4 MΩ, WPI Inc., Sarasota, FL), the signal was amplified 100x (AM Systems, Sequim, WA), further amplified with a custom-made amplifier 300–500x, filtered (high pass 200 Hz; low pass 10,000 Hz; Krohn-Hite, Brockton, MA) and digitized with a custom-made A-to-D converter for analysis. Tonotopic mapping was performed to confirm that we identified primary auditory cortex (AI) using criteria that subdivided mouse auditory cortex into five auditory areas including AI (Steibler, 1997). Specifically, AI was characterized by units exhibiting sharp tuning, short first spike latency, no adaptation, and systematic changes in the spatial frequency organization (Sally and Kelly, 1988). Injections were made into AI using a cocktail of Fluorogold (hydroxystilbamidine, Biotium, Inc., Hayward, California) and biotinylated dextran amine (BDA) by passing 5 μA of alternating current for 3–8 minutes. The wounds were closed with sutures, antibiotics and analgesics were administered, and the animals were allowed to recover.

Histology

Following a 6–10 day survival, mice were given a lethal injection of pentobarbital (100 mg/kg, IP). When the subject was areflexic to corneal stimulation, transcardial perfusion with paraformaldehyde 3–4% (in 0.1 M phosphate buffer, pH 7.4) was performed. The mice were decapitated and the heads post-fixed for 1–3 hours. The brains were then removed from the cranial vault. The forebrain was isolated and the cerebral hemispheres separated from the underlying thalamus. Each hemisphere was cryoprotected in a buffered solution of 30% sucrose for several days, flattened on a freezing microtome stage, sectioned at a thickness of 50 μm, and collected in buffer in serial order. These sections were coverslipped in buffer and photographed using a fluorescent microscope to localize the injection site. Then the coverslips were removed and the tissue histochemically reacted for cytochrome oxidase using standard techniques (Wong-Riley, 1979). Analysis revealed that each cortical injection site was centered within the cytochrome oxidase staining region of temporal cortex (Fig. 8), confirming that primary auditory cortex was successfully targeted (Wallace, 1987).

Each thalamus from experimental mice was embedded in gelatin-albumin, cut on a Vibratome at 50 μm thickness, and coverslipped with Krystalon. This procedure permitted analysis of the distribution of retrogradely labeled cells in the medial geniculate body (MGB) where distribution plots demonstrated that nearly all cells were confined to the ventral division of the MGB (Fig. 9). These data offered additional support that injections were located within AI (Ryugo and Killackey, 1974;Oliver and Hall, 1978;Morel and Imig, 1987;Romanski and LeDoux, 1993;Winer et al., 1999).

Cross sections through the cochlear nuclei were taken at 50 μm thickness. Histological processing for BDA was performed as previously described (Doucet and Ryugo, 1997). Briefly, sections were rinsed in buffer, incubated overnight in ABC solution (5° C, Vector Elite Kit, Vector Labs, Burlingame, CA), and reacted with diaminobenzidine using standard techniques to reveal the reaction product. One set of sections was mounted on gelatin-coated microscope slides, coverslipped, and photographed. A second set of sections was processed for analysis using electron microscopy as described previously (Weedman and Ryugo, 1996b). Sections for electron microscopic analysis were placed in a solution of 1% osmium tetroxide for 15 minutes, stained en bloc with 1% uranyl acetate, dehydrated, infiltrated with Epon, and embedded between two sheets of Aclar. After photographing and drawing labeled fibers with a drawing tube, labeled boutons of interest were embedded in BEEM capsules, cut at 70 nm thickness, placed on Formvar coated slotted grids, and analyzed with a Hitachi (Model H-7600-I) transmission electron microscope.

Results

We demonstrate that primary auditory cortex has direct bilateral projections to the GCD of the cochlear nucleus. Primary auditory cortex was physiologically identified using short first spike latency, sharp tuning, no adaptation, and tonotopic organization as criteria (Sally and Kelly, 1988). The location of the injection site was histologically verified because it was centered in the region darkly stained for cytochrome oxidase, and retrogradely labeled cells from this site were distributed within the ventral division of the medial geniculate body, the known source of thalalmocortical afferents to AI. These data provided important controls for proceeding with analysis of the cortical projections to the cochlear nucleus.

The magnitude of the projection to either side was variable between cases with no side being dominant. Labeled fibers were observed largely in the granule cell lamina between the DCN and VCN, the superficial lamina along the dorsolateral edge of the VCN, the subpeduncular corner which is a region beneath the inferior cerebellar peduncle, lateral to the spinal tract of the trigeminal and medial to the dorsal VCN, and diffusely throughout the DCN (Fig. 10). Fibers ran predominantly along the surface of the CN, but occasionally ran orthogonal to the surface. Frequent fiber branching was observed. Occasionally, long fibers arose from a branch point with many *en passant* swellings (Fig. 10C). *En passant* swellings varied in size from 1–3 μm. Despite extensive efforts to identify a particular swelling under the electron microscope that was seen with the light microscope, it was common to find more labeled swellings using electron microscopy than were detected with the light microscope. This situation revealed the superior resolving power of the electron microscope. It should also be noted that it was difficult to differentiate between *en passant* and terminal swellings because they were similar in size and structure, and the incoming and outgoing axon segments were not always observed for *en passant* swellings.

Electron microscopic examination of the labeled endings demonstrated that they formed asymmetric synapses with dendritic profiles typical of granule cells (Fig. 11). The labeled terminals contained round synaptic vesicles, one or several mitochondria, and were found both ipsilateral (Fig. 11A, B) and contralateral (Fig. 11C, D) to the injection site. One synapse per labeled bouton ending was observed, and there were no obvious structural differences between the ipsilateral and contralateral projection. These synapses terminated on thin dendrites, at least some of which also received inputs from endings containing pleiomorphic synaptic vesicles, similar to the observations in rat (Fig. 6). Postsynaptic dendrites were characterized by the presence of mitochondria, a loose intracellular matrix, microtubules, and an absence of synaptic vesicles. They often gave rise to fine hairs that penetrated labeled cortical terminal. These dendritic features are characteristic of terminal granule cell dendrites.

Discussion

Electrophysiologic methods were used to identify primary auditory cortex (AI) for anterograde tracer injections, and histologic methods were used to verify the placement and to confirm that they tracer did not spread beyond the AI borders. The resulting new data from the mouse confirmed and extended what has been reported for the rat (Weedman and Ryugo, 1996b) and guinea pig (Schofield and Coomes, 2005). Thus a generalized plan for corticofugal projections from auditory cortex to cochlear nucleus may be inferred. Within the GCD, there are a number of cell types but the main one for our purposes is the granule cell (Mugnaini et al., 1980b). This neuron has a small cell body with scant cytoplasm, gives rise to several thin straight dendrites that terminate in a claw-like structure, and emits an unmyelinated axon that traverses layer I of the DCN perpendicular to the tonotopic axis. Enclosed within these dendritic claws are mossy fiber endings that arise from the cuneate and spinal trigeminal nuclei (Wright and Ryugo, 1996; Haenggeli et al., 2005). Located on the tips of the dendrites are terminals that arise from auditory cortex and terminals of unknown origin that contain pleiomorphic synaptic vesicles (Fig. 11). Glial lamellae are also associated with this synaptic complex.

Primary auditory cortex in mouse and rat gives rise to a diffuse projection of small bouton endings to granule cell dendrites of the GCD of the cochlear nucleus. These boutons produce a single synapse that is remote from the cell body. The impact of the corticobulbar fibers on these granule cells is unknown but is probably modulatory in nature. Their role may be postulated in light of evidence that the GCD is the recipient of inputs from different neural sources, including somatosensory, vestibular, and motor (Ryugo et al., 2003). This arrangement suggests that the GCD, modulated by multimodal input, impacts neural encoding of auditory information at the level of the cochlear nucleus. Auditory cortical input could directly effect coding properties of CN neurons as has been shown for somatosensory inputs on the response tuning properties of neurons in the CN (Davis et al., 1996; Kanold and Young, 2001; Oertel and Young, 2004). In any case, cortical feedback must be considered when one tries to understand how the auditory system functions.

The survival advantage for selective listening as an outgrowth of a larger neocortex is undeniable. A corollary to this idea would be to test whether the magnitude of descending projections increases in accordance with the increase in neocortical tissue. An organism must be able to distinguish and separate the auditory features of a predator from an auditory scene if they are to avoid becoming prey. A collateral advantage of selective listening is its associated contribution to spoken language and the ability to make fine auditory distinctions. As agrarian culture gave way to populated city centers, the capacity to follow a conversation in a noisy crowd resulted from the brain’s capacity to segregate sound streams. Biological systems with such capabilities should have the feature where the listener’s expectations and subsequent predictions will “tune” the ear to the expected sounds. Is this facility evident in the human ability of active listening to music? The capacity to appreciate distinct but simultaneous musical elements in a symphonic performance suggests a complex neural network that shapes expectations about melodic, rhythmic, and aesthetic elements. The cortico-cochlear nucleus projection may be one element of the neural network that enables these complex listening functions. It is exactly these kinds of functions that promote the study of neural systems in an attempt to understand the brain and the mind.

Acknowledgments

This work was supported by NIH grants RO1 DC04395 and T32 DC00027. The authors gratefully thank Tan Pongstaphone and Karen Montey for technical assistance, and John Doucet for helpful discussions of the data.

Grant Sponsor: National Institutes of Health; Grant Numbers: RO1 DC04395, T32 DC00027

Literature cited

Davis KA, Miller RL, Young ED. Effects of somatosensory and parallel-fiber stimulation on neurons in dorsal cochlear nucleus. J Neurophysiol. 1996; 76:3012–3024. [PubMed: 8930251]

Doucet JR, Molavi DL, Ryugo DK. The source of corticocollicular and corticobulbar projections in area Te1 of the rat. Exp Brain Res. 2003; 153:461–466. [PubMed: 13680047]

Doucet JR, Ryugo DK. Projections from the ventral cochlear nucleus to the dorsal cochlear nucleus in rats. J Comp Neurol. 1997; 385:245–264. [PubMed: 9268126]

Feliciano M, Saldaña E, Mugnaini E. Direct projections from the rat primary auditory neocortex to nucleus sagulum, paralemniscal regions, superior olivary complex and cochlear nuclei. Aud Neurosci. 1995; 1:287–308.

Floris A, Diño M, Jacobowitz DM, Mugnaini E. The unipolar brush cells of the rat cerebellar cortex and cochlear nucleus are calretinin-positive: A study by light and electron microscopic immunocytochemistry. Anat Embryol. 1994; 189:495–520. [PubMed: 7978355]

Haenggeli CA, Pongstaporn T, Doucet JR, Ryugo DK. Projections from the spinal trigeminal nucleus to the cochlear nucleus in the rat. J Comp Neurol. 2005; 484:191–205. [PubMed: 15736230]

Kanold PO, Young ED. Proprioceptive information from the pinna provides somatosensory input to cat dorsal cochlear nucleus. J Neurophysiol. 2001; 21:7848–7858.

Morel A, Imig TJ. Thalamic projections to fields A, AI, P, and VP in the cat auditory cortex. J Comp Neurol. 1987; 265:119–144. [PubMed: 2826552]

Mugnaini E, Osen KK, Dahl AL, Friedrich VL Jr, Korte G. Fine structure of granule cells and related interneurons (termed Golgi cells) in the cochlear nuclear complex of cat, rat, and mouse. J Neurocytol. 1980a; 9:537–570. [PubMed: 7441303]

Mugnaini E, Warr WB, Osen KK. Distribution and light microscopic features of granule cells in the cochlear nuclei of cat, rat, and mouse. J Comp Neurol. 1980b; 191:581–606. [PubMed: 6158528]

Oertel D, Young ED. What's a cerebellar circuit doing in the auditory system? Trends Neurosci. 2004; 27:104–110. [PubMed: 15102490]

Oliver DL, Hall WC. The medial geniculate body of the tree shrew, Tupaia glis. II. Connections with the neocortex. J Comp Neurol. 1978; 182:459–493. [PubMed: 102661]

Romanski LM, LeDoux JE. Organization of rodent auditory cortex: anterograde transport of PHA-L from MGv to temporal neocortex. Cereb Cortex. 1993; 3:499–514. [PubMed: 7511011]

Ryugo DK, Haenggeli CA, Doucet JR. Multimodal inputs to the granule cell domain of the cochlear nucleus. Exp Brain Res. 2003; 153:477–485. [PubMed: 13680048]

Ryugo DK, Killackey HP. Differential telencephalic projections of the medial and ventral divisions of the geniculate body of the rat. Brain Res. 1974; 82:173–177. [PubMed: 4611594]

Sally SL, Kelly JB. Organization of auditory cortex in the albino rat: sound frequency. J Neurophysiol. 1988; 59:1627–1638. [PubMed: 3385476]

Schofield BR, Coomes DL. Auditory cortical projections to the cochlear nucleus in guinea pigs. Hear Res. 2005; 199:89–102. [PubMed: 15574303]

Stiebler I, Neulist R, Fichtel I, Ehret G. The auditory cortex of the house mouse: left-right differences, tonotopic organization and quantitative analysis of frequency representation. J Comp Physiol [A]. 1997; 181:559–571.

Tuchmann-Duplessis, H.; Auroux, M.; Haegel, P. Illustrated Human Embryology. In: Hurley, LS., translator. Nervous System and Endocrine Glands. Vol. Volume III. New York: Spring-Verlag; 1975. Translated by

Wallace MN. Histochemical demonstration of sensory maps in the rat and mouse cerebral cortex. Brain Res. 1987; 418:178–182. [PubMed: 2822205]

Weedman DL, Pongstaporn T, Ryugo DK. Ultrastructural study of the granule cell domain of the cochlear nucleus in rats: Mossy fiber endings and their targets. J Comp Neurol. 1996; 369:345–360. [PubMed: 8743417]

Weedman DL, Ryugo DK. Pyramidal cells in primary auditory cortex project to cochlear nucleus in rat. Brain Res. 1996a; 706:97–102. [PubMed: 8720496]

Weedman DL, Ryugo DK. Projections from auditory cortex to the cochlear nucleus in rats: Synapses on granule cell dendrites. J Comp Neurol. 1996b; 371:311–324. [PubMed: 8835735]

Weisberg JA, Rustioni A. Cortical cells projecting to the dorsal column nuclei of cats. An anatomical study with the horseradish peroxidase technique. J Comp Neurol. 1976; 168:425–437. [PubMed: 950388]

Weisberg JA, Rustioni A. Cortical cells projecting to the dorsal column nuclei of rhesus monkeys. Exp Brain Res. 1977; 28:521–528. [PubMed: 408162]

Weisberg JA, Rustioni A. Differential projections of cortical sensorimotor areas upon the dorsal column nuclei of cats. J Comp Neurol. 1979; 184:401–421. [PubMed: 762290]

Winer JA, Sally SL, Larue DT, Kelly JB. Origins of medial geniculate body projections to physiologically defined zones of rat primary auditory cortex. Hear Res. 1999; 130:42–61. [PubMed: 10320098]

Wong-Riley M. Changes in the visual system of monocularly sutured or enucleated cats demonstrable with cytochrome oxidase histochemistry. Brain Res. 1979; 171:11–28. [PubMed: 223730]

Wright DD, Ryugo DK. Mossy fiber projections from the cuneate nucleus to the cochlear nucleus in the rat. J Comp Neurol. 1996; 365:159–172. [PubMed: 8821448]

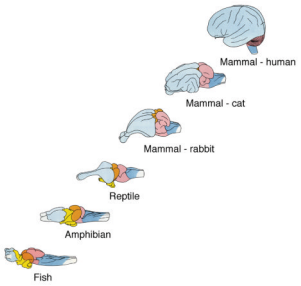

Figure 1.
Diagram illustrating the relative growth of the cerebral hemispheres along a phylogenetic line of vertebrates. The brains are not drawn to scale. Note that the spinal cord and brain stem remain somewhat constant. It is this growth of the neocortex which is hypothesized to endow mammals (and humans) their large behavioral capacity and evolutionary advantage. Modified from Tuchmann-Duplessis, Auroux and Haaegel, 1975.

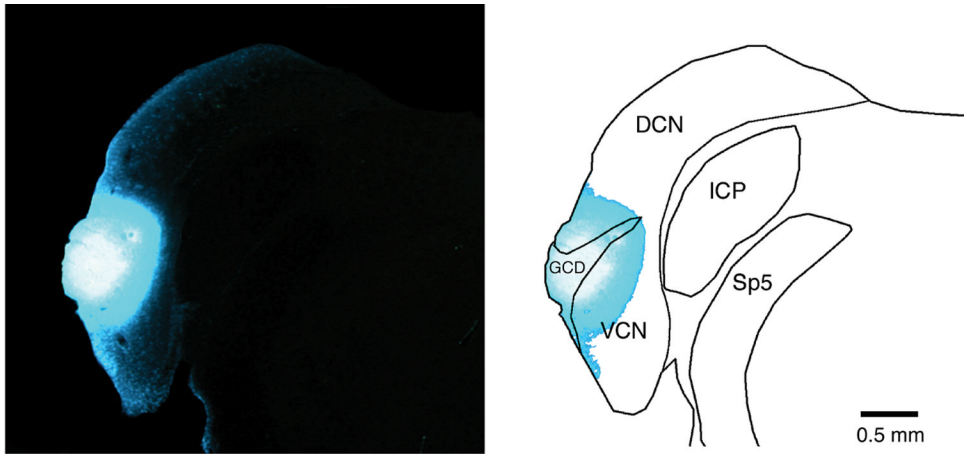

Figure 2.
Photomicrograph of fluorescent injection site of Fast Blue (left panel) and drawing (right side) that illustrate its confinement to the cochlear nucleus. This injection is typical of those used in these studies. Abbreviations: DCN, dorsal cochlear nucleus; GCD, granule cell domain; ICP, inferior cerebellar peduncle; VCN, ventral cochlear nucleus; Sp5, spinal tract of the trigeminal.

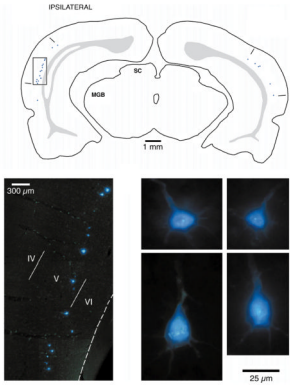

Figure 3.
Drawing (top) of coronal section through the forebrain of a rat illustrating the location of retrogradely labeled cortical neurons as a result of an injection of Fast Blue in the cochlear nucleus. The ipsilateral labeling is stronger than that on the contralateral side. The box indicates the location of the fluorescent photomicrograph (lower left) with the Fast Blue labeled neurons located in the deep part of layer V. High magnification photomicrographs of labeled pyramidal cells (4 panels on lower right). Modified from figure 6 of Doucet et al., 2002.

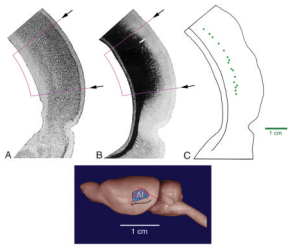

Figure 4.
Cyto- and myeloarchitecture of primary auditory cortex (AI). Photomicrograph of Nissl-stained section (far left) shows area with high cell density in layer IV (marked by arrows and purple lines). Myelin-stained section (middle panel) illustrates that AI has high myelin content from thalalmocortical afferents. Distribution of retrogradely labeled neurons from a cochlear nucleus injection (far right) occurs in a cortical region that coincides with the architectonic fields of AI. The reconstruction and projection of these fields onto a side view of the brain (bottom panel) shows the topical location of AI. This region conforms to the site that was defined as primary auditory cortex (black dots for recording sites, red lines for blood vessels, and black line for rhinal fissure) using electrophysiological methods (Sally and Kelley, 1988). The top panels were modified from Weedman and Ryugo, 1996a.

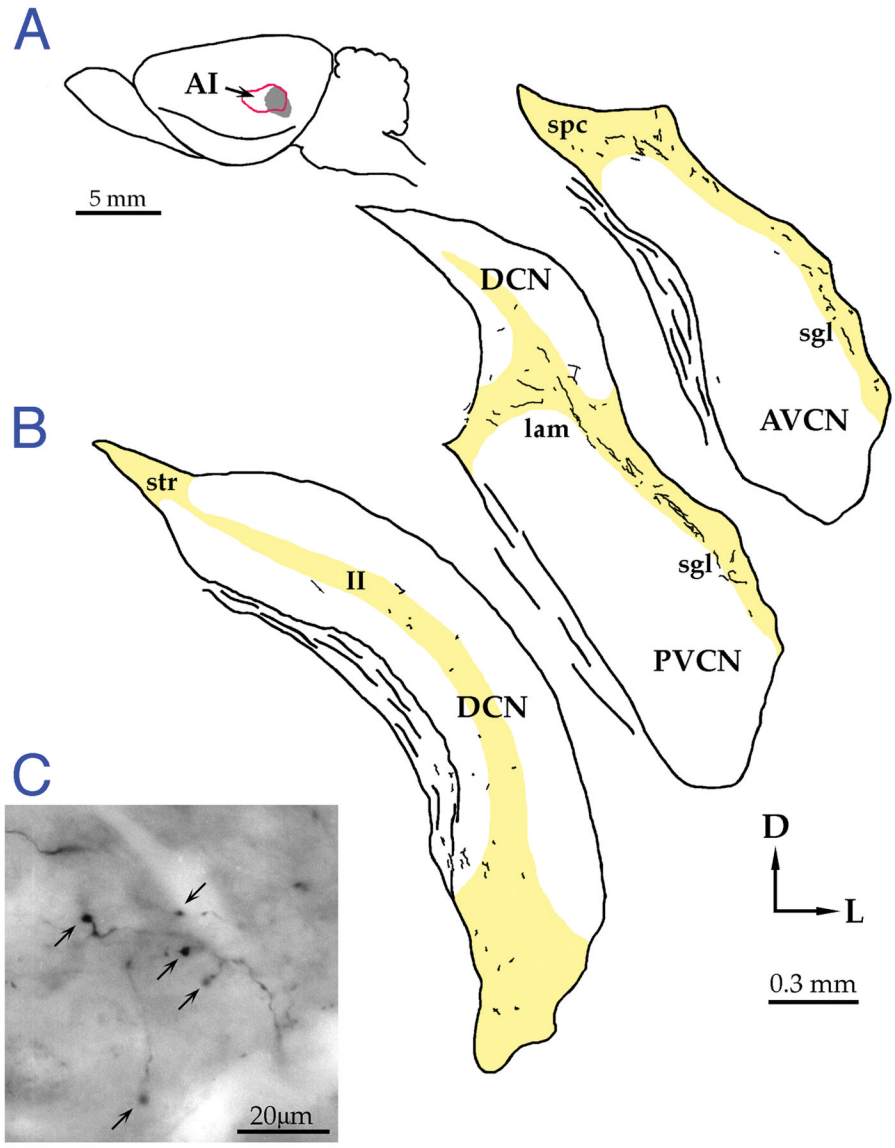

Figure 5.
Distribution of cortico-cochlear nucleus fibers and terminals in the rat. (A) Drawing illustrates injection site. (B) Coronal sections through the cochlear nucleus showing that the projections (indicated in black) are found almost entirely within the granule cell domain (yellow). (C) Photomicrograph of BDA-labeled fibers and terminals. Taken from Weedman and Ryugo, 1996b.

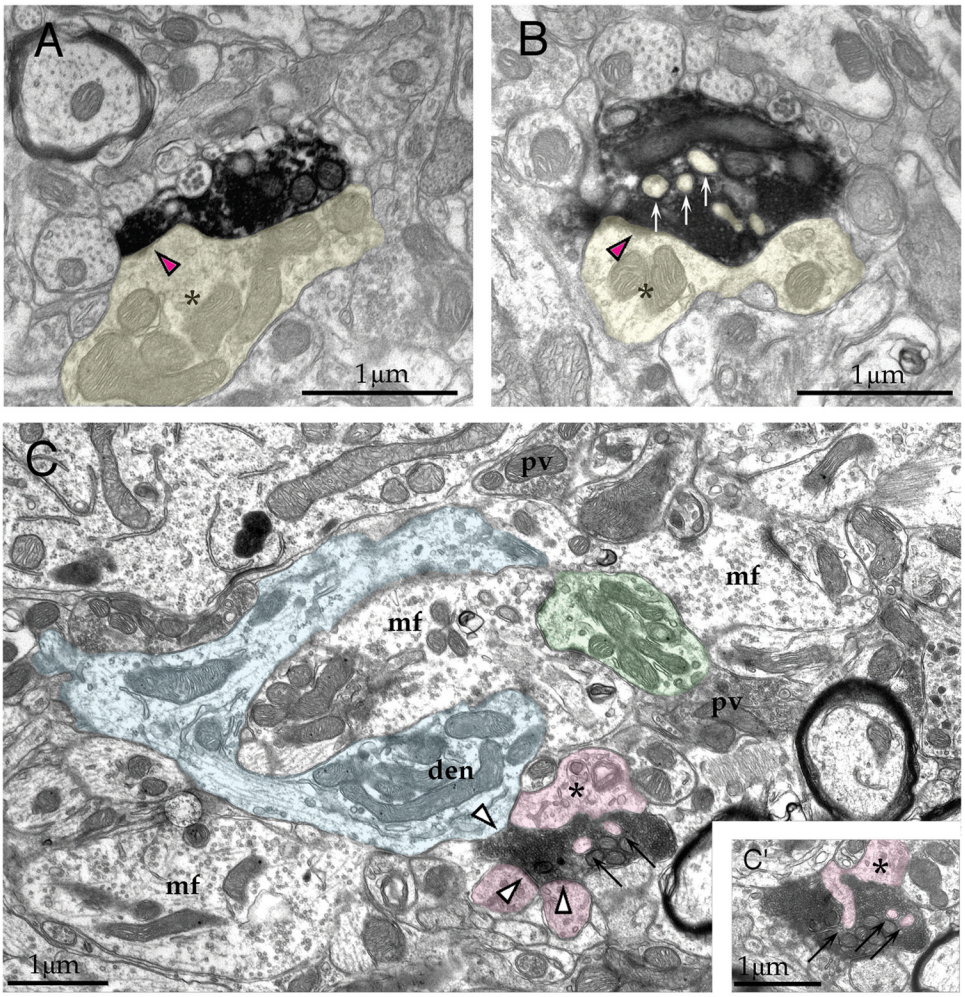

Figure 6.
Electron micrographs illustrating labeled cortical terminals synapsing (arrowheads) onto thin dendrites (marked by asterisks and colored yellow, pink, blue and green). Fine dendritic "hairs" penetrate the cortical endings (arrows in B and C). A mossy fiber (mf) is clutched by a granule cell claw (C) and the claw is in turn postsynaptic to a cortical terminal. The data show that corticobulbar terminals are on "remote" sites on granule cells. Modified from Weedman and Ryugo, 1996b.

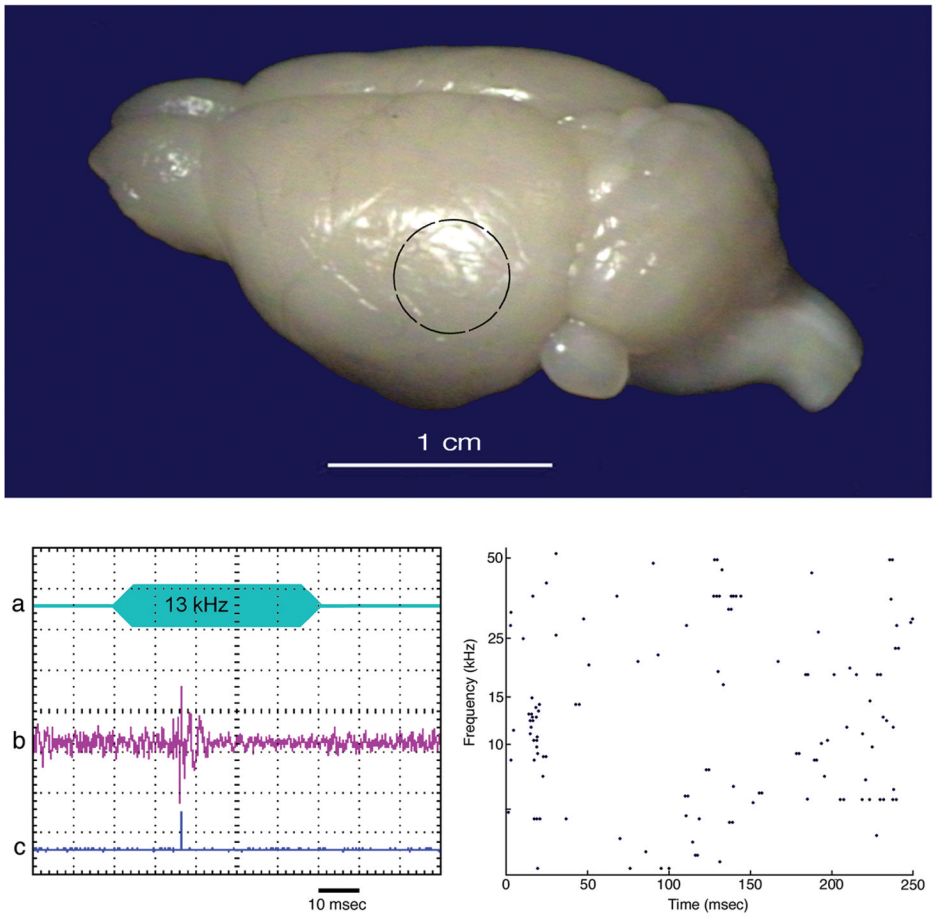

Figure 7.

Photograph of mouse brain from a posterolateral view (top panel). The black circle indicates the region that was sampled by recording microelectrodes. (Lower left) Oscilloscope tracings of (a) stimulus, (b) output of microelectrode, and (c) output of the Schmitt trigger. The 13 kHz tone evoked a transient spike train. (Lower right) Raster plot of spikes recorded over 250 msec to 50 msec tone bursts of different frequencies. The evoked spikes occurred in response to tones of 8.5–14 kHz, with the best response coming from 13 kHz. These electrophysiological data identified primary auditory cortex so injections of BDA could be made with confidence.

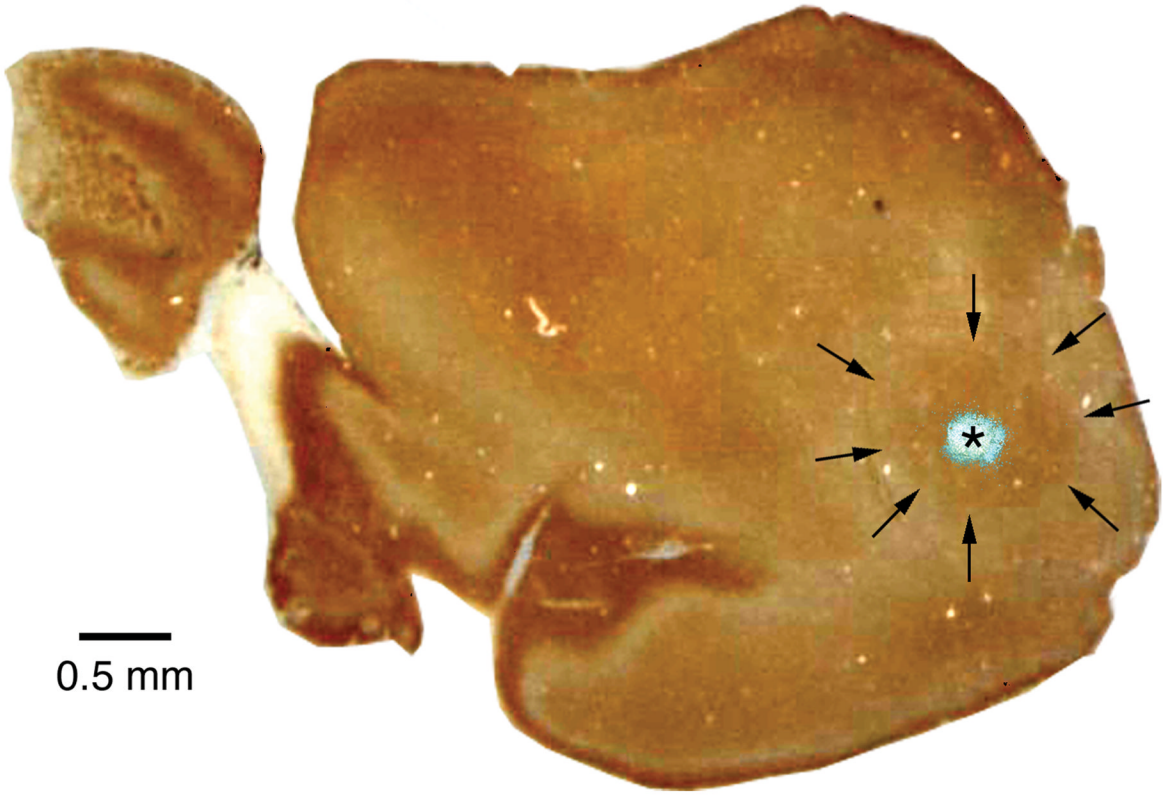

Figure 8.
Photomicrograph of flattened cortical section, stained for cytochrome oxidase, with the FlouroGold injection site superimposed. The fluorescent photomicrograph was taken before cytochrome oxidase staining. The brown reaction product of cytochrome oxidase, marking AI, lies in the posterolateral region of cortex and is indicated by arrows. Rostral is to the left, medial is to the top.

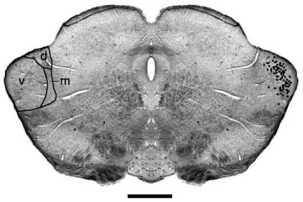

Figure 9.
Photomicrograph of unstained section through the medial geniculate body (MGB) located in the caudal thalamus. When sections are mounted in buffer and illuminated by diffuse light, myelinated fibers appear dark and yield a pattern of fiber architecture that reveals the main subdivisions of the MGB. The locations of fluorescently labeled neurons from an AI injection were concentrated in the ventral division of the MGB (v) and are indicated by black dots. Abbreviations: d, dorsal division of MGB; m, medial division of MGB. Scale bar equals 0.5 mm.

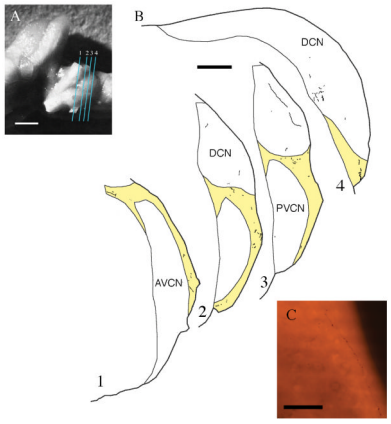

Figure 10.

Distribution of corticobulbar projections to the cochlear nucleus. A. Photograph of mouse brain stem from a lateral view. The near-vertical lines indicate the orientation plane of the sections shown in B. Scale bar equals 1 mm. (B) Drawings of tissue sections with plots of labeled fibers and terminals. Most of the projection is distributed in the GCD (yellow) with some diffuse projections to the DCN. Scale bar equals 200 μm. (C) Photomicrograph of BDA-labeled fiber with numerous *en passant* swellings. This fiber with *en passant* swellings traverses layer I of the DCN and eventually dips down into layer II to give off terminal swellings. Scale bar equals 100 μm.

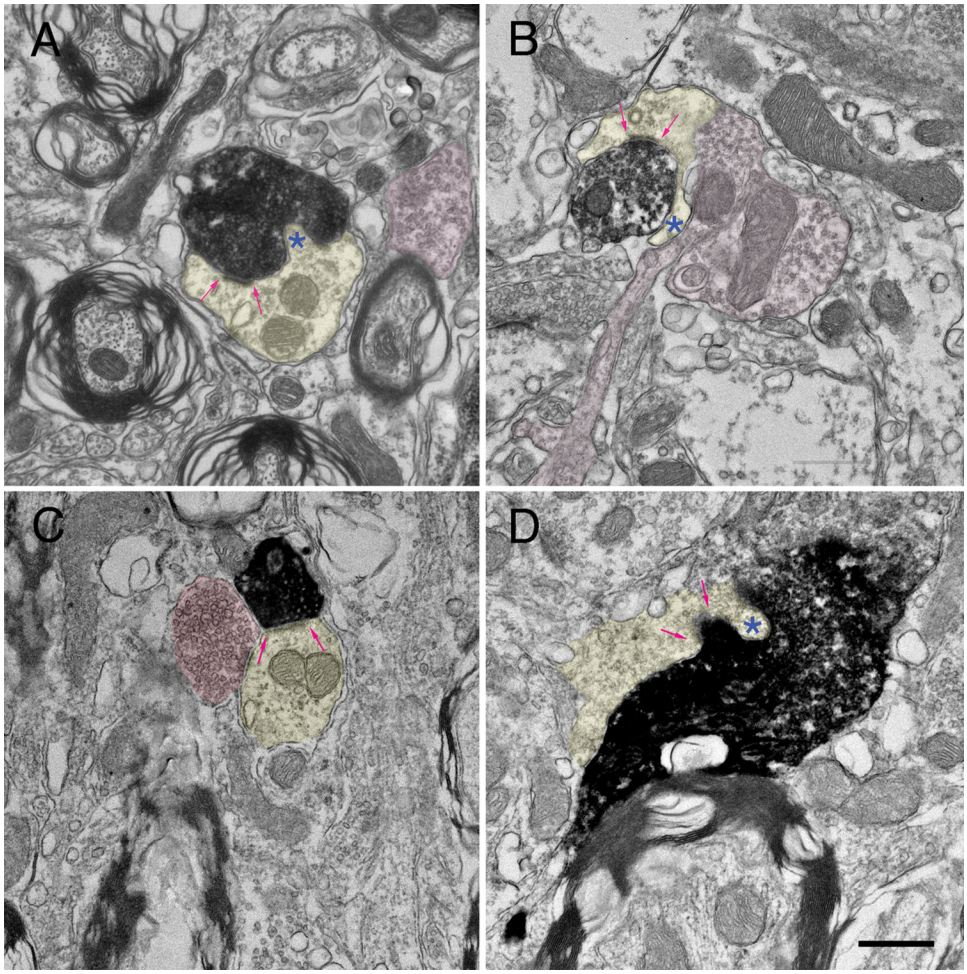

Figure 11.
Electron micrographs of labeled cortical terminals in the ipsilateral (A, B) and contralateral (C, D) GCD of the cochlear nucleus. The labeled endings contain round synaptic vesicles and form asymmetric contacts (arrows) with thin dendrites (yellow). These dendrites often give rise to hair-like protuberances (*) that penetrate the afferent ending. Frequently, these dendrites are also contacted by terminals containing pleiomorphic synaptic vesicles (pink). The features of these postsynaptic dendrites are typical of granule cells. Scale bar equals 0.5 μm.

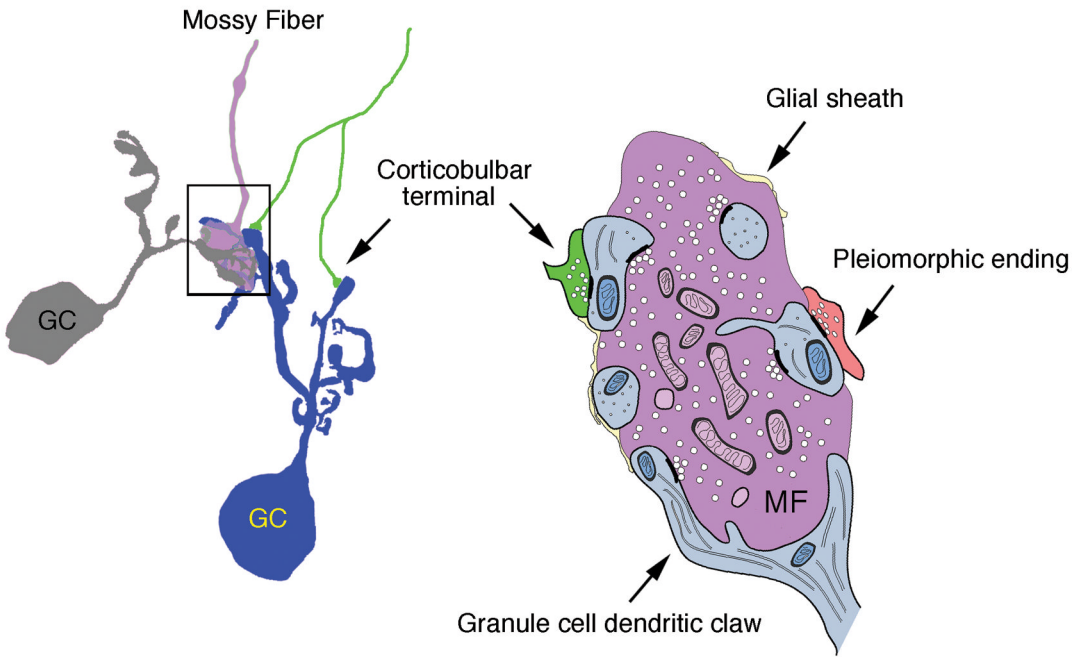

Figure 12.
Summary diagram of the synaptic glomerulus contributed to by mossy fibers, granule cell dendrites, and corticobulbar endings. The small size and remote location of the cortical terminals suggest that the postsynaptic effect is modulatory.